Part II: Bulk metallic glasses

May 19th 2009

H. Franz

Summary

Glasses are materials with amorphous structure showing a gradual transition from the liquid to the solid without well defined melting point

Structure similar to the liquid

Mode coupling theory is describing the essentials of this transition

Bulk Metallic Glasses

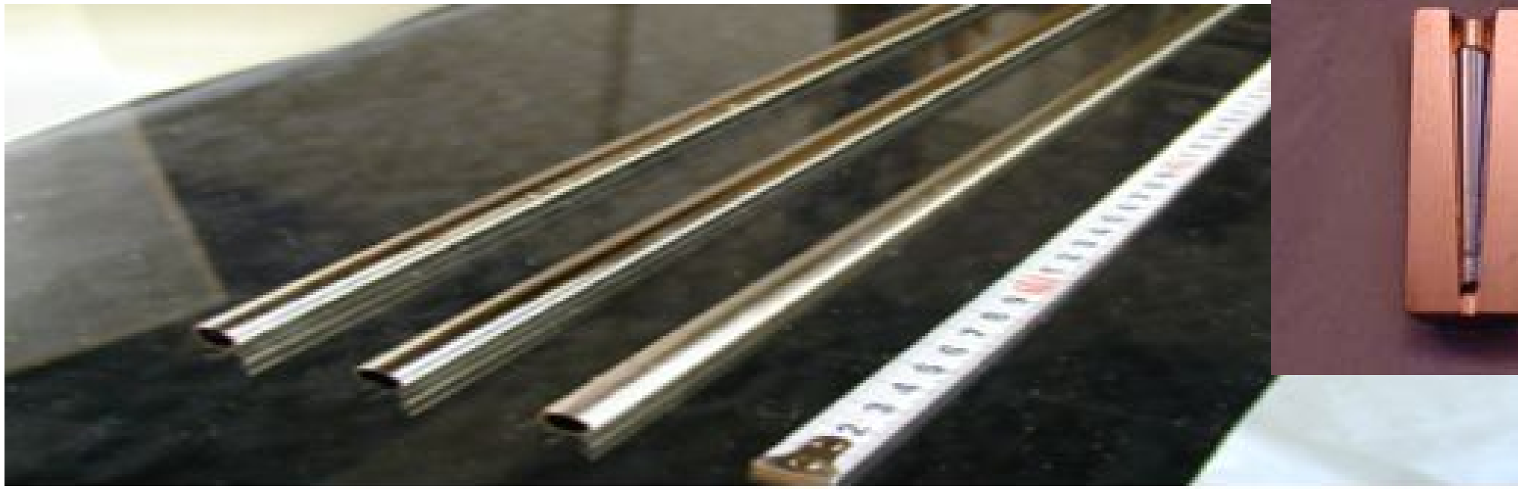

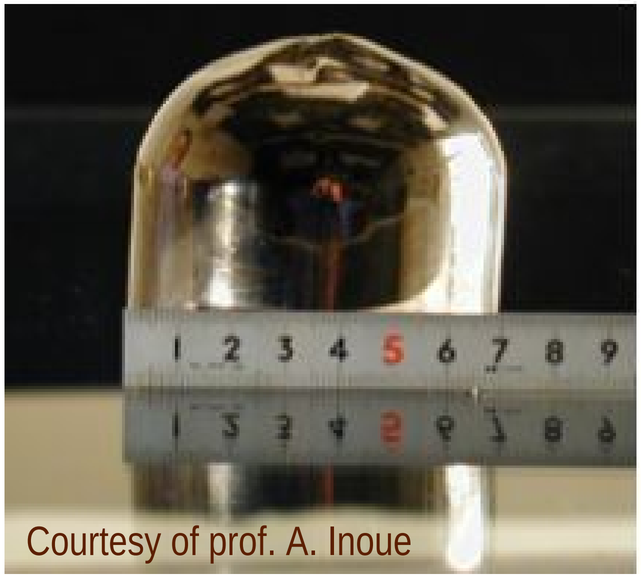

Courtesy of prof. A. Inoue

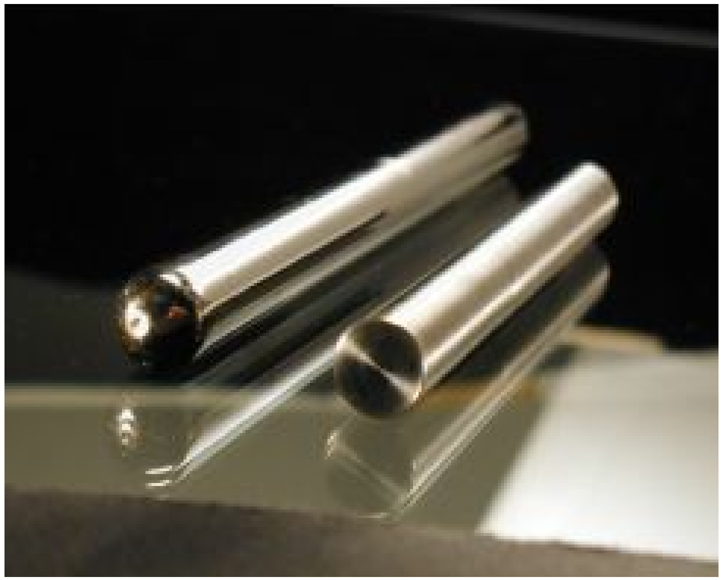

Systems

- Historically first alloy AuSi (1960) cooling with 10^6 K/s
- 1969 PdCuSi – only 10^3 K/s needed
- First commercial amorphous alloy, Vitreloy 1 (41.2% Zr, 13.8% Ti, 12.5% Cu, 10% Ni, 22.5% Be)
- Families of alloys
  - Pd based: PdCuNiP
  - Zr based: ZrNi, ZrTiCuNiBe (v4), ZrAlNiCuAg, ZrPd, ZrAlCu, ZrAlCuNiFe
  - La based
  - Fe based: FePCAlBGa
  - Cu based: CuZr, CuTiZr
  - Al based: AlLaNi
  - Ni based: NiZr, NiNbY

  - and many more

Systems

Table 1
The critical sizes (d_c) and thermal parameters for $Zr_{100-x-y}(Cu_zAg_{1-z})_yAl_x$ ($x = 7$–9 at.%, $y = 42$–50 at.% and $z = 0.75$–0.875) alloys, together with other BMGs reported in Refs. [20,27,28] for comparison

Alloys	Critical size	Amorphous ingots (25 g)	T_g	T_x	T_m	T_l	ΔT_x	T_{rg}	γ
$Zr_{46}Cu_{46}Al_8$	5 mm	No	715	771	978	1163	56	0.615	0.411
$Zr_{47}(Cu_{4/5}Ag_{1/5})_{46}Al_7$	<20 mm	No	704	783	1055	1242	79	0.567	0.402
$Zr_{47}(Cu_{4.5/5.5}Ag_{1/5.5})_{46}Al_7$	<20 mm	Partial	702	782	1056	1123	80	0.625	0.428
$Zr_{47}(Cu_{5/6}Ag_{1/6})_{46}Al_7$	<20 mm	Partial	703	781	1060	1125	78	0.625	0.427
$Zr_{47}(Cu_{6/7}Ag_{1/7})_{46}Al_7$	20 mm	Partial	709	774	1057	1118	65	0.634	0.424
$Zr_{45}(Cu_{4/5}Ag_{1/5})_{48}Al_7$	20 mm	Partial	710	783	1062	1208	73	0.588	0.408
$Zr_{45}(Cu_{4.5/5.5}Ag_{1/5.5})_{48}Al_7$	>20 mm	Yes	711	785	1063	1154	74	0.616	0.421
$Zr_{45}(Cu_{5/6}Ag_{1/6})_{48}Al_7$	>20 mm	Yes	713	786	1061	1159	73	0.615	0.420
$Zr_{43}(Cu_{5/6}Ag_{1/6})_{50}Al_7$	20 mm	No	738	770	1075	1127	32	0.65	0.413
$Zr_{50}(Cu_{4/5}Ag_{1/5})_{42}Al_8$	20 mm	Partial	703	774	1089	1155	71	0.609	0.417
$Zr_{50}(Cu_{5/6}Ag_{1/6})_{42}Al_8$	<20 mm	Partial	701	764	1095	1138	63	0.616	0.415
$Zr_{48}(Cu_{3/4}Ag_{1/4})_{44}Al_8$	20 mm	Partial	706	770	1092	1218	64	0.580	0.400
$Zr_{48}(Cu_{4/5}Ag_{1/5})_{44}Al_8$	>20 mm	Yes	707	762	1090	1132	55	0.625	0.414
$Zr_{48}(Cu_{4.5/5.5}Ag_{1/5.5})_{44}Al_8$	>20 mm	Yes	706	777	1089	1129	71	0.625	0.423
$Zr_{48}(Cu_{5/6}Ag_{1/6})_{44}Al_8$	>20 mm	Yes	705	778	1090	1122	73	0.628	0.426
$Zr_{48}(Cu_{6/7}Ag_{1/7})_{44}Al_8$	>20 mm	Yes	706	778	1089	1127	72	0.626	0.424
$Zr_{48}(Cu_{7/8}Ag_{1/8})_{44}Al_8$	20 mm	Partial	707	779	1095	1127	72	0.627	0.425
$Zr_{46}(Cu_{4/5}Ag_{1/5})_{46}Al_8$	>20 mm	Yes	710	776	1091	1228	66	0.578	0.400
$Zr_{46}(Cu_{4.5/5.5}Ag_{1/5.5})_{46}Al_8$	>20 mm	Yes	703	775	1088	1126	72	0.624	0.424
$Zr_{46}(Cu_{4.5/5.5}Ag_{1/5.5})_{46}Al_8$ ingots	>20 mm	Yes	704	776	1089	1130	72	0.623	0.423
$Zr_{46}(Cu_{5/6}Ag_{1/6})_{46}Al_8$	>20 mm	Partial	710	778	1088	1120	68	0.634	0.425
$Zr_{53}(Cu_{5/6}Ag_{1/6})_{38}Al_9$	20 mm	Partial	711	767	1089	1129	56	0.63	0.417
$Zr_{51}(Cu_{4.5/5.5}Ag_{1/5.5})_{40}Al_9$	20 mm	Partial	703	758	1092	1144	55	0.615	0.410
$Zr_{49}(Cu_{5/6}Ag_{1/6})_{42}Al_9$	20 mm	Partial	708	767	1092	1242	59	0.57	0.393
$Cu_{43}Zr_{43}Al_7Ag_7$ [27]	8 mm	–	722	794	1125	–	72	–	–
$Zr_{41.2}Ti_{13.8}Cu_{12.5}Ni_{10}Be_{22.5}$ [28]	25 mm	–	623	672	932	996	49	0.67	0.415
$Pd_{40}Cu_{30}Ni_{10}P_{20}$ [28]	72 mm	–	575	670	804	840	95	0.72	0.473
$La_{62}Al_{14}Cu_{11.3}Ag_{2.7}Ni_5Co_5$ [20]	>20 mm	–	422	482	642	727	60	0.580	0.419
$La_{65}Al_{14}Cu_{9.2}Ag_{1.8}Ni_5Co_5$ [20]	35 mm	–	419	459	641	687	40	0.610	0.415

"Yes", "partial" and "no" are roughly defined by eyes for ingots having volume fractions of larger than about 80%, 30–80% and less than about 30% for the amorphous component, respectively.

Favorable conditions for glass formation

Couple of empirical rules in literature

However up to now still empirical (trail and error) development

- **Three or more alloy components**
- **Very different atomic radii**
- **Negative heat of mixing**
- **Low eutectic**
- **Competing crystalline phases**

Structure vs. macroscopic properties

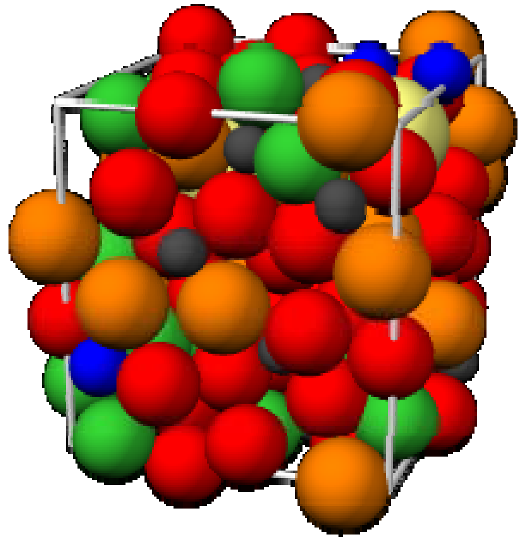

Understanding relation between the structure and macroscopic properties is important for improving performance of existing and crucial for designing novel materials

Applications

Transformers

low thermal losses

Light weight compounds in space crafts

high specific strength

Surface coating

very hard thin films

Magnetic properties

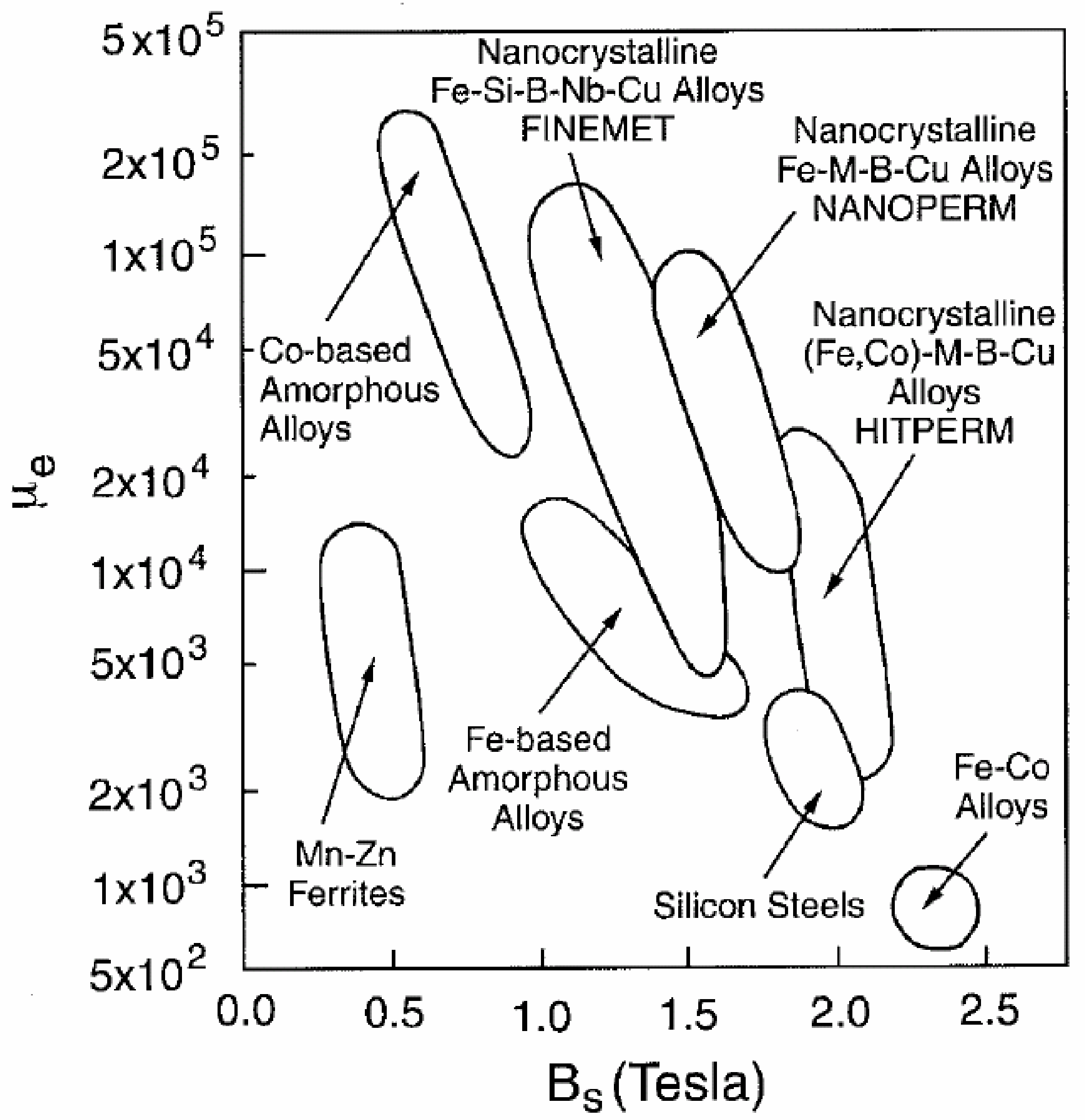

High strength

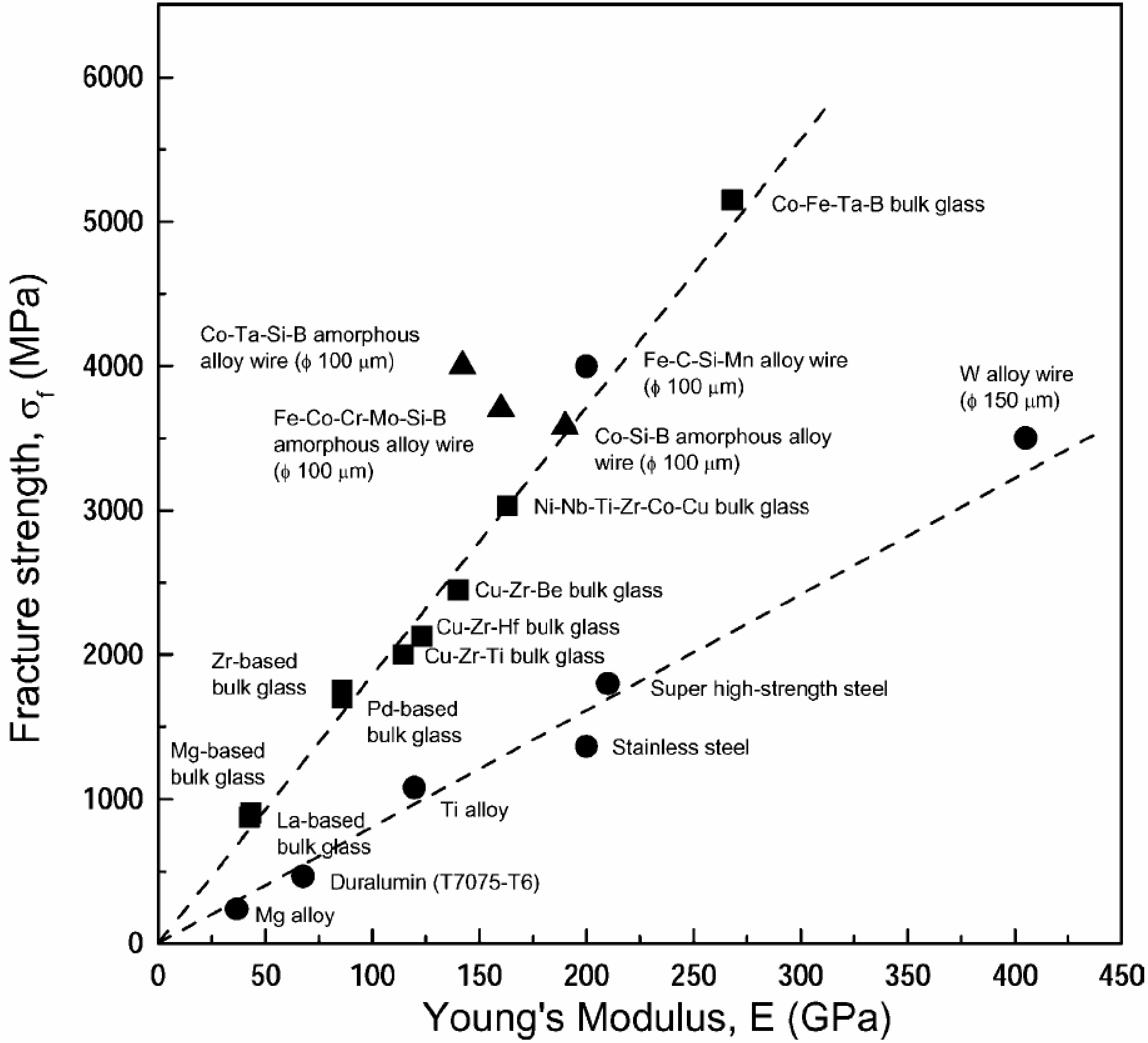

Sample preparation - melt spinning

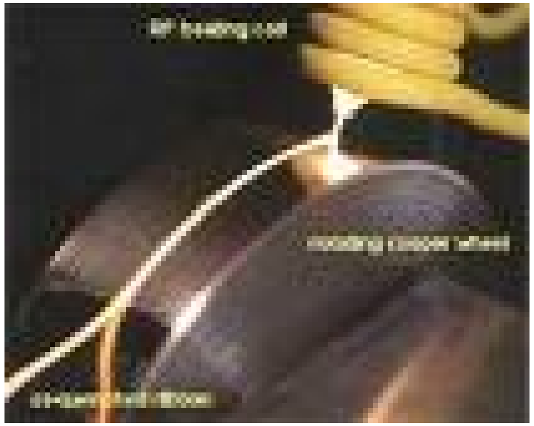

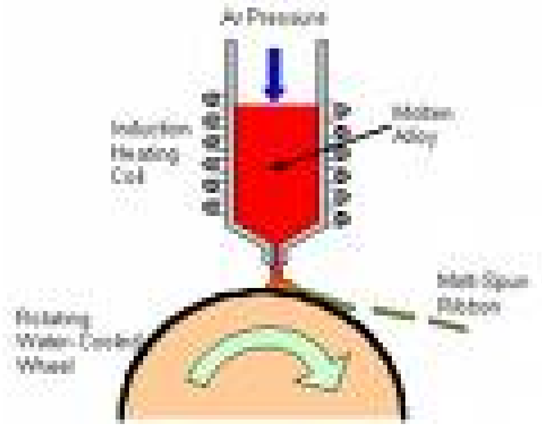

Rather wide spread

Cooling rate up to 10^5 K/s

Production of large quantities

However only thin films (couple of 10 μm)

Sample preparation - splat cooling

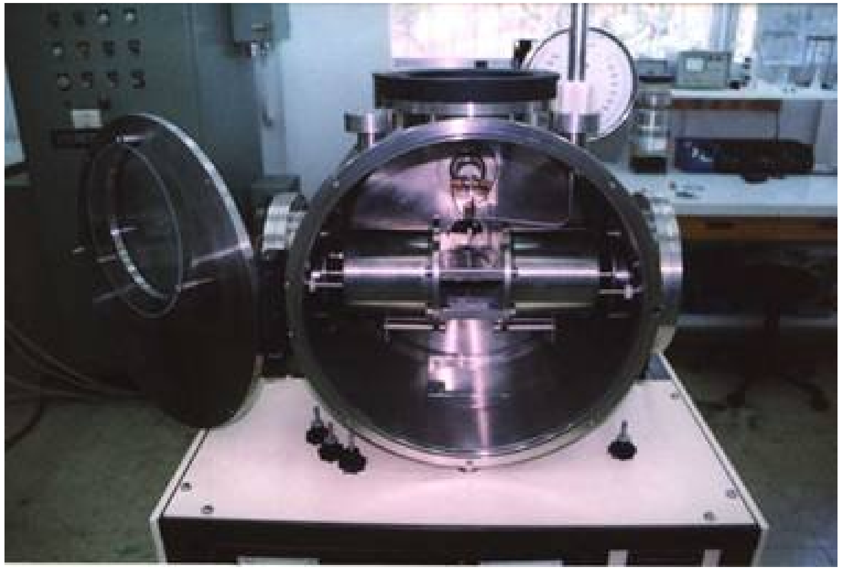

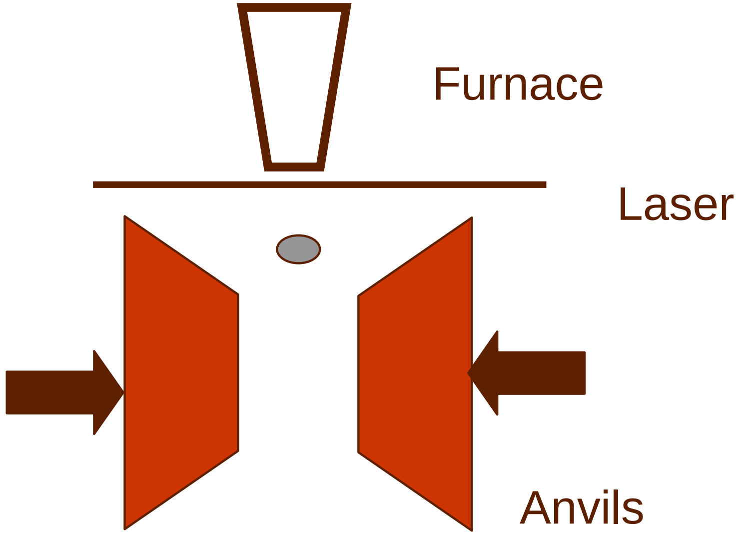

Rather wide spread

Cooling rate up to 10^6 K/s

Production of small quantities

Only thin disks (couple of 10 μm)

In-situ tensile experiments

Tensile/compression module

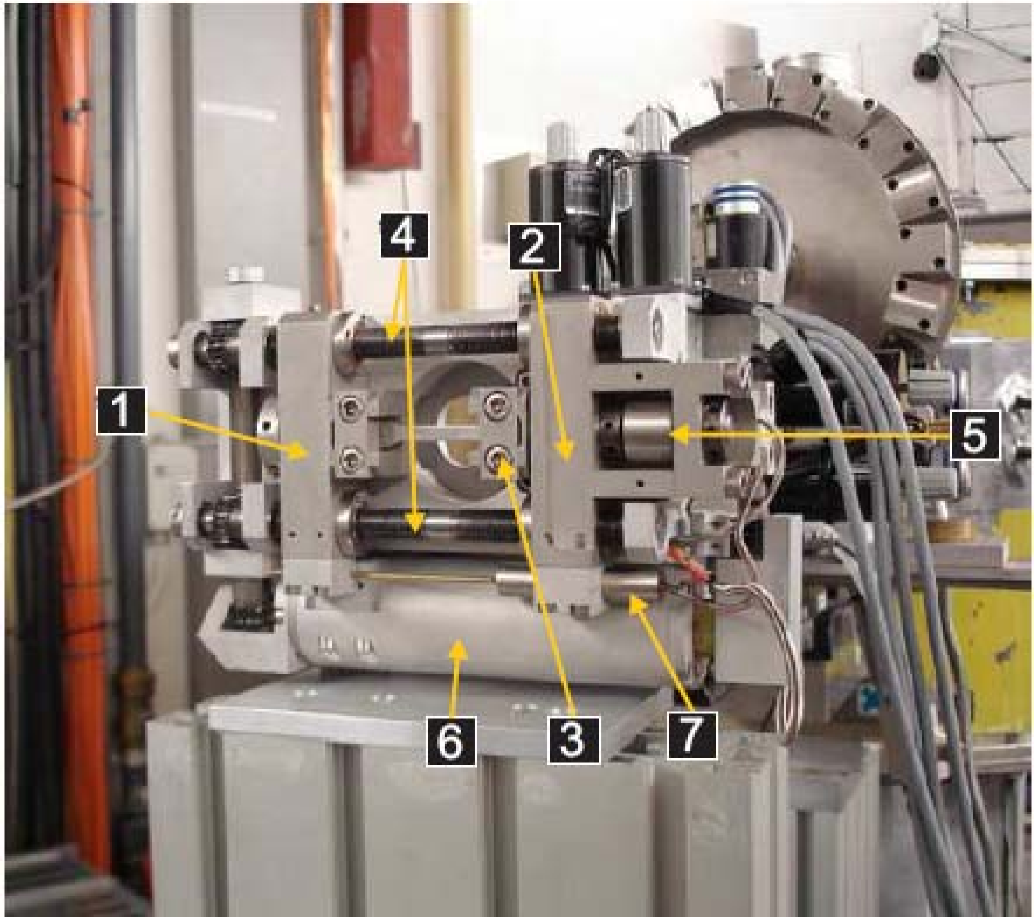

[1] - rear yoke, [2] - front yoke, [3] - clamping,
[4] - leading screws, [5] -load cell, [6] - motor,
[7] - displacement gauge

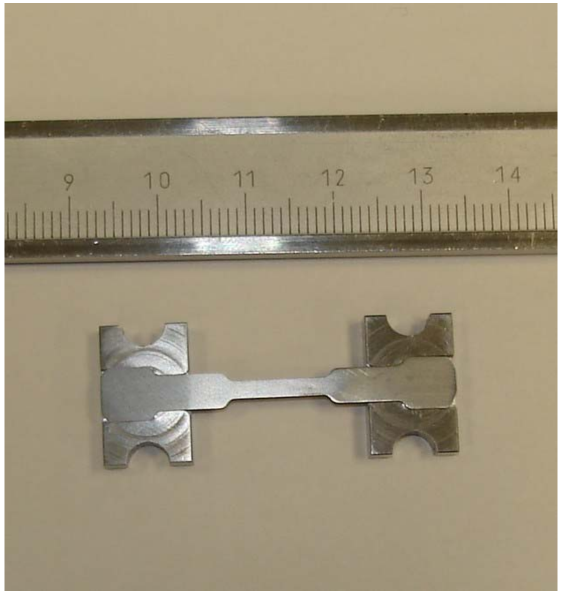

$Zr_{64.13}Cu_{15.75}Ni_{10.12}Al_{10}$

Y. H. Liu, G. Wang, R. J. Wang, D. Q. Zhao, M. X. Pan, and W. H. Wang, Science **315**, 1385 2007.

Storage ring DORIS III

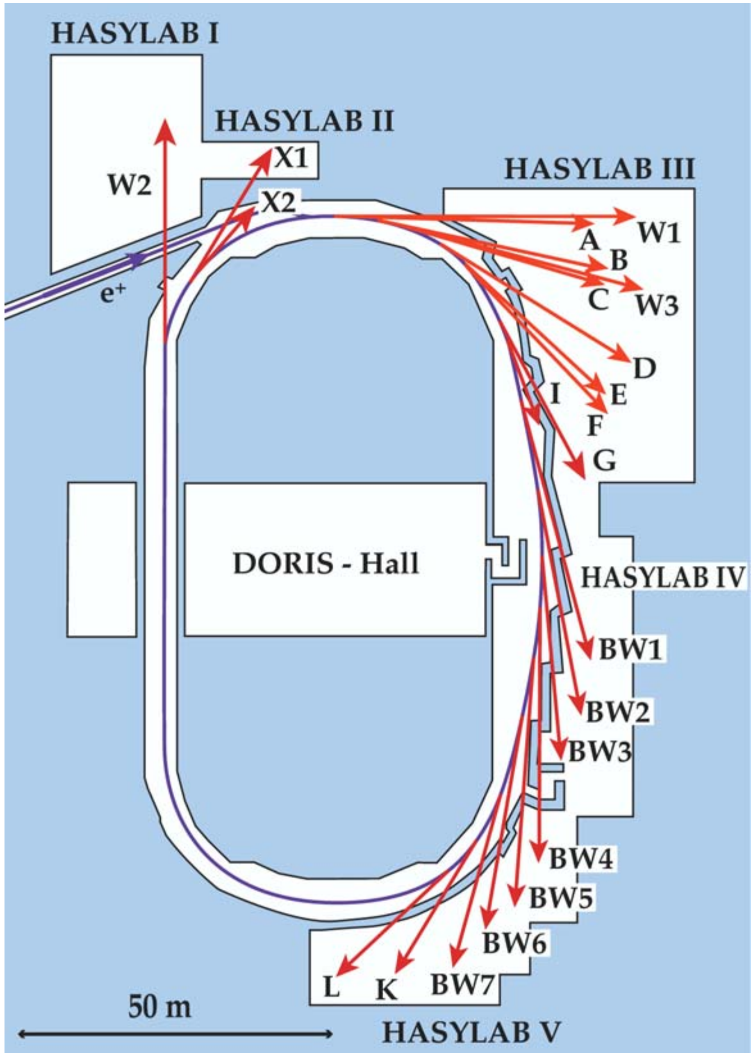

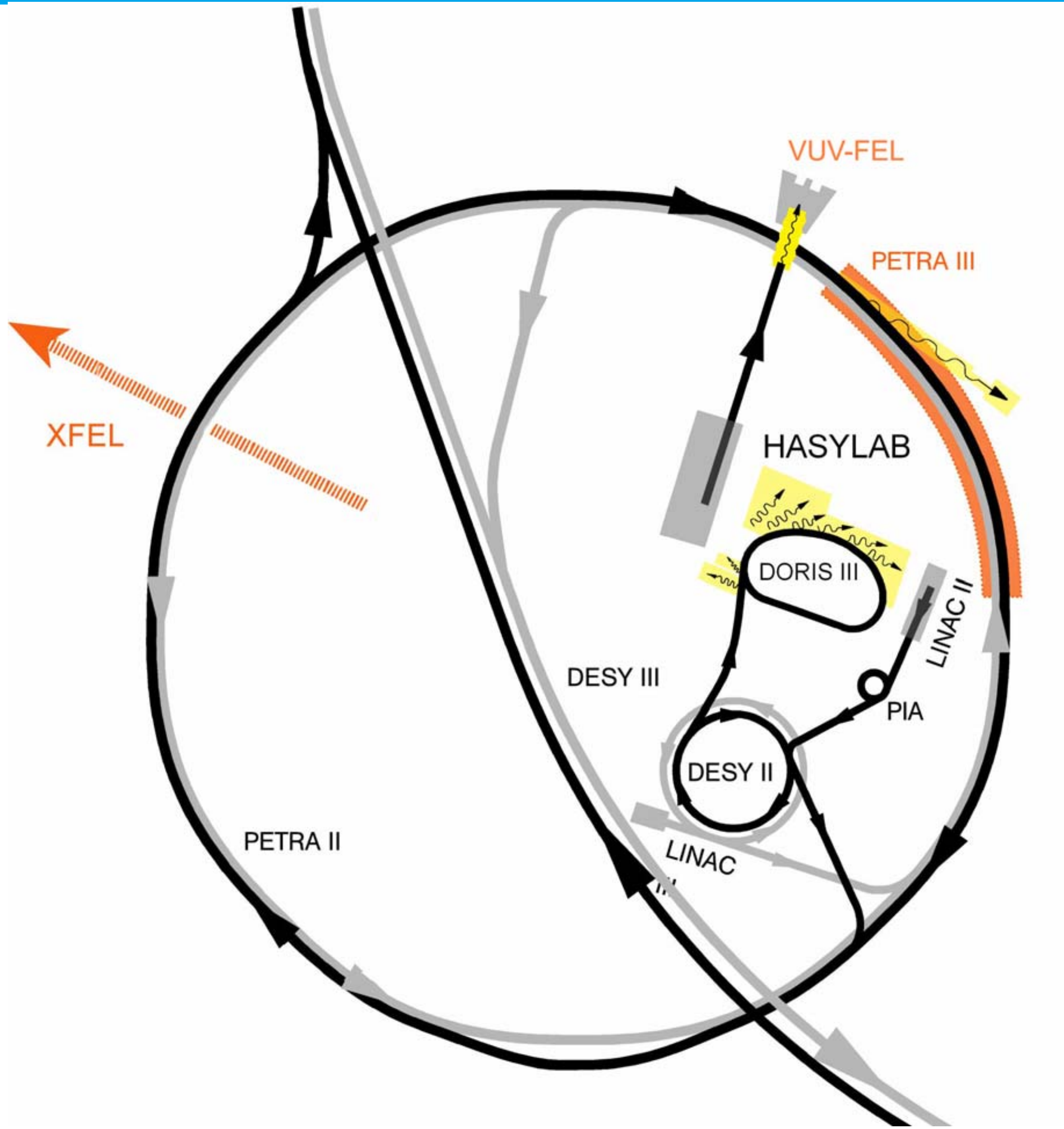

In-situ tensile experiments using high-energy XRD

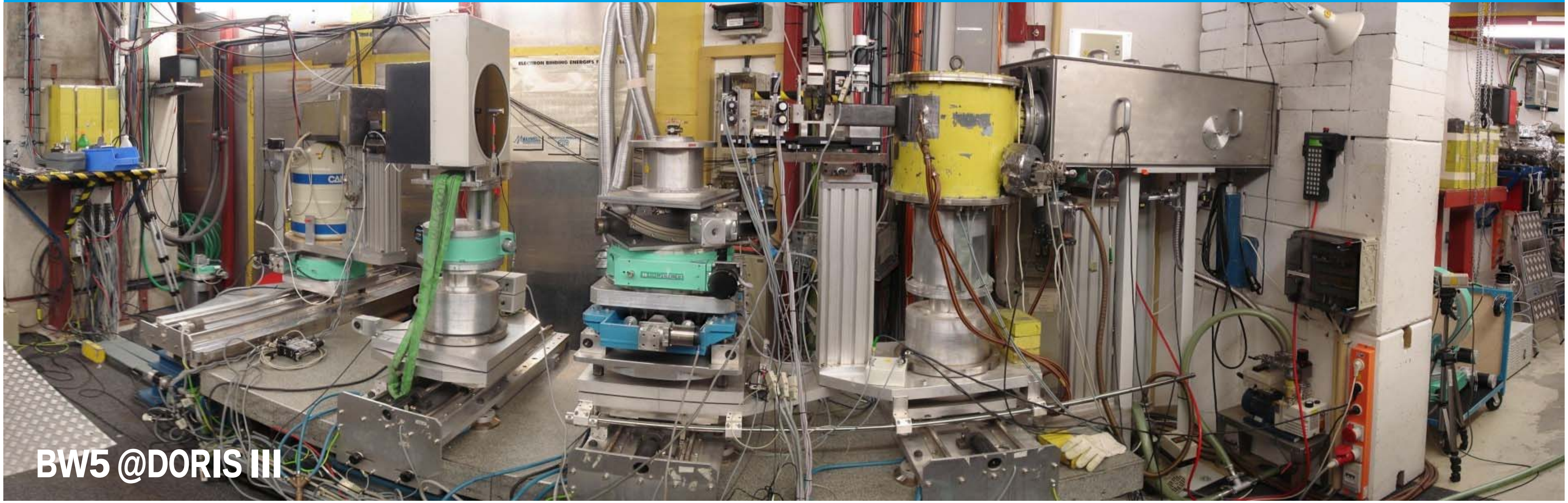

BW5 is dedicated to X-ray scattering experiments using high-energy photons (**60 - 150 keV**).

The **large penetration depth** at these energies of typically **sereral mm to cm** allows the investigation of bulk materials and complex sample environments.

The experimental station is equipped with a triple axis diffractometer and an **image plate** camera.

Parameters:

- wavelength λ = 0.12398 Å (100 keV)
- crossection of collimated beam 1mm^2
- exposure time 10 s
- XRD in transmission mode
- 2D ma345 image plate detector used in symetric mode

In-situ tensile experiments

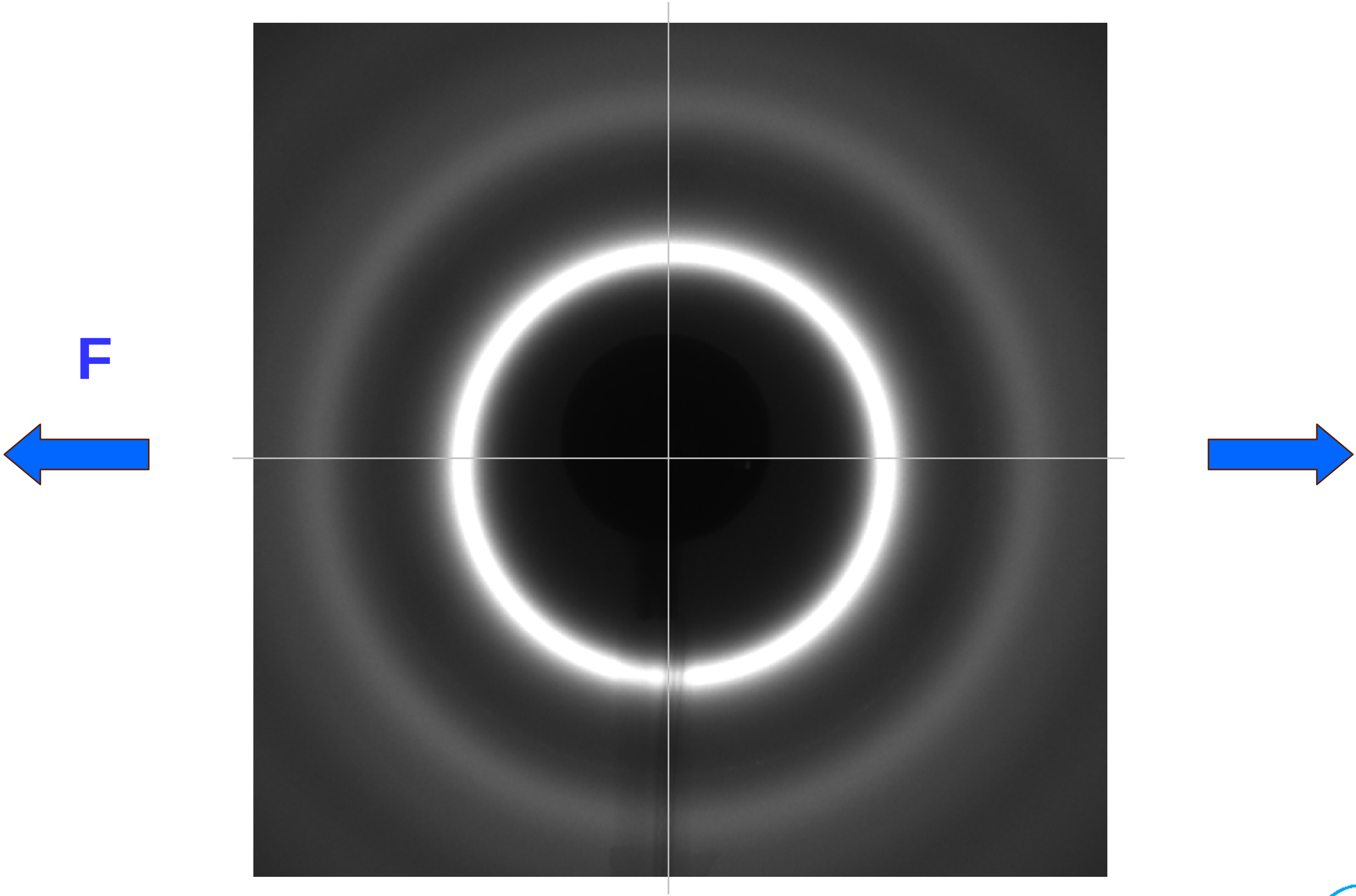

Courtesy J. Bednarcik

Determination of deformation state by XRD

The symmetric circular diffraction pattern is characterized with respect to the polar coordinates (*s*, η). By dividing the η-range of 0 to 2π into 36 segments, one obtains symmetrized intensity distributions

$$I'_i(Q,\eta_i) = \int_{\eta_i-\pi/36}^{\eta_i+\pi/36} \left[I(Q,\eta) + I(Q,\eta+\pi)\right] d\eta$$

with $i = 1\ldots18$, where the wave-vector transfer $Q = Q(s)$ is defined by

$$Q(s) = \frac{4\pi}{\lambda}\sin\left(\frac{1}{2}\,arctg\left(\frac{s}{D}\right)\right)$$

in which λ denotes the wavelength, D refers to the sample-to-detector distance and s represents the distance from the origin of the polar coordinate system.

The relative change of the position of the principal peak upon applying an external stress defines the strain

$$\varepsilon_i(\eta_i,\sigma) = \frac{q(\eta_i,0) - q(\eta_i,\sigma)}{q(\eta_i,\sigma)}$$

H. F. Poulsen et al., *Nat. Mater.* **4** 33-35 (2005)

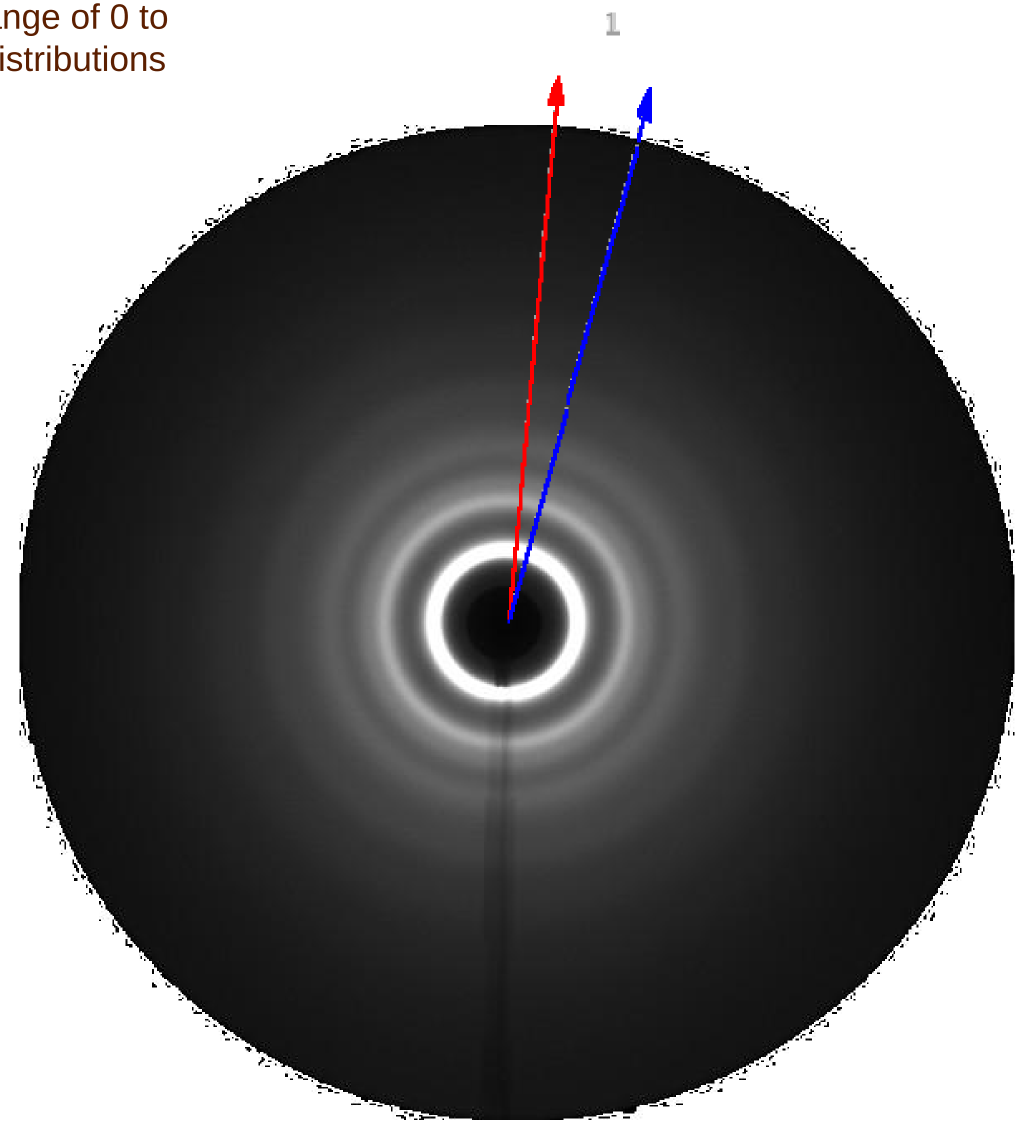

Determination of tensor components

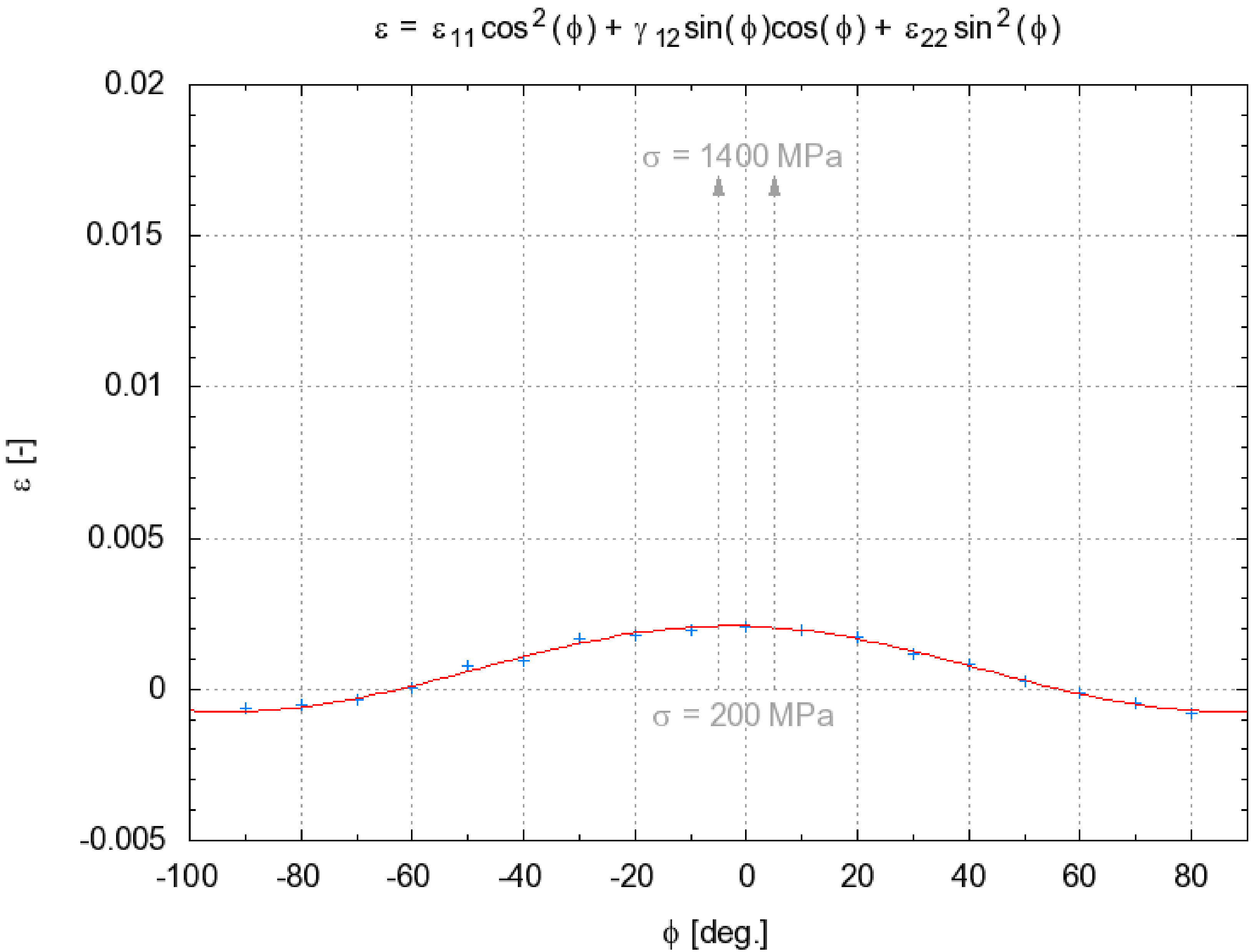

Analysis in reciprocal space

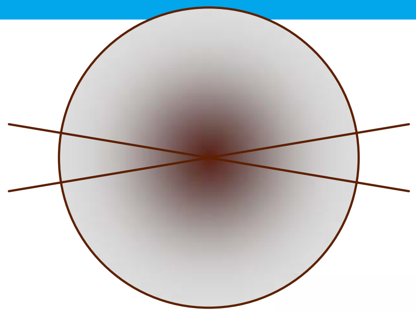

$$S(Q) = 1 + \frac{I_e(Q) - \left[\sum_{i=1}^{n} c_i f_i^2(Q)\right]}{\left[\sum_{i=1}^{n} c_i f_i(Q)\right]^2}$$

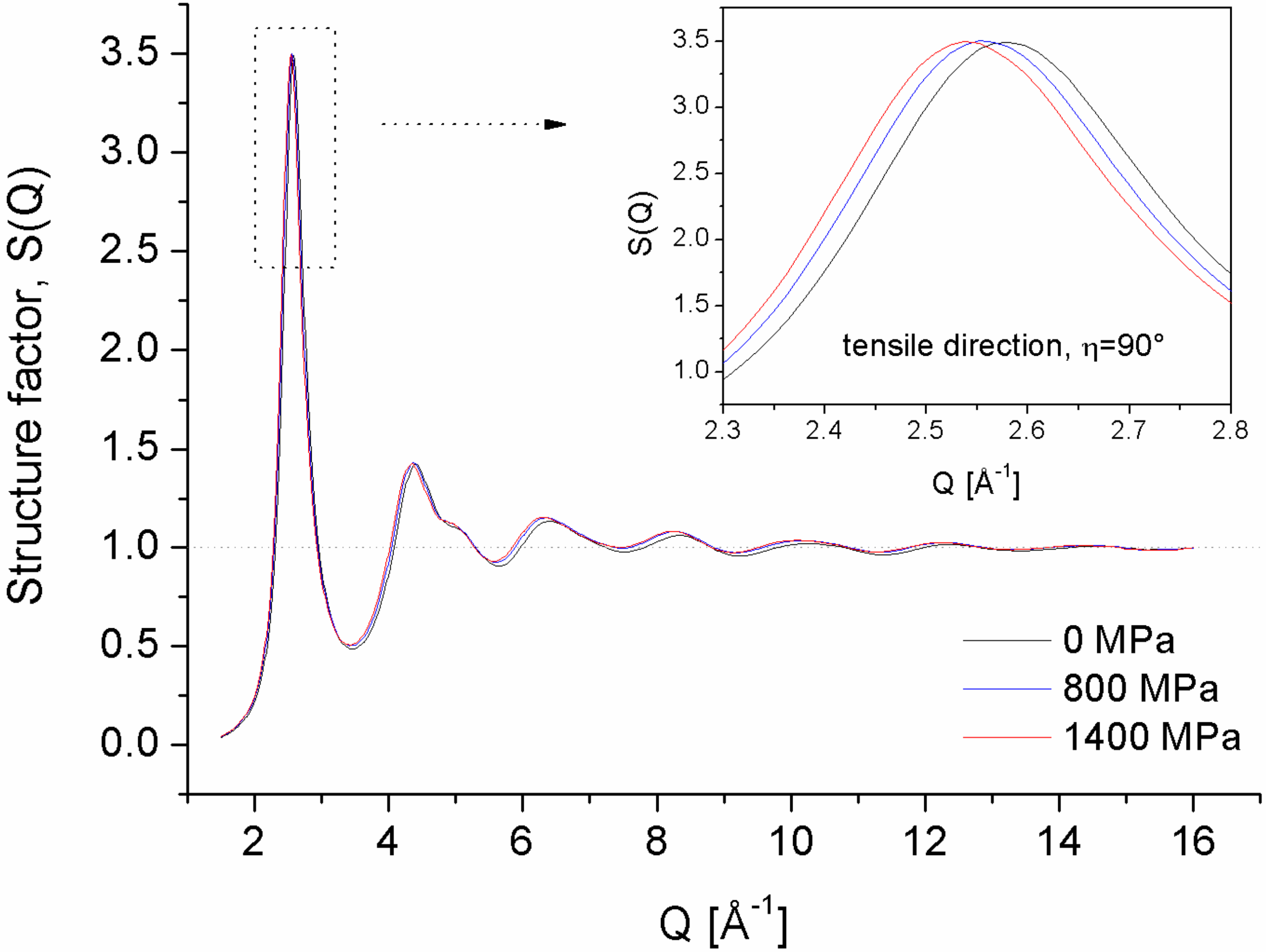

Stress-strain curves

La based metallic glass

Only elastic strain !!!

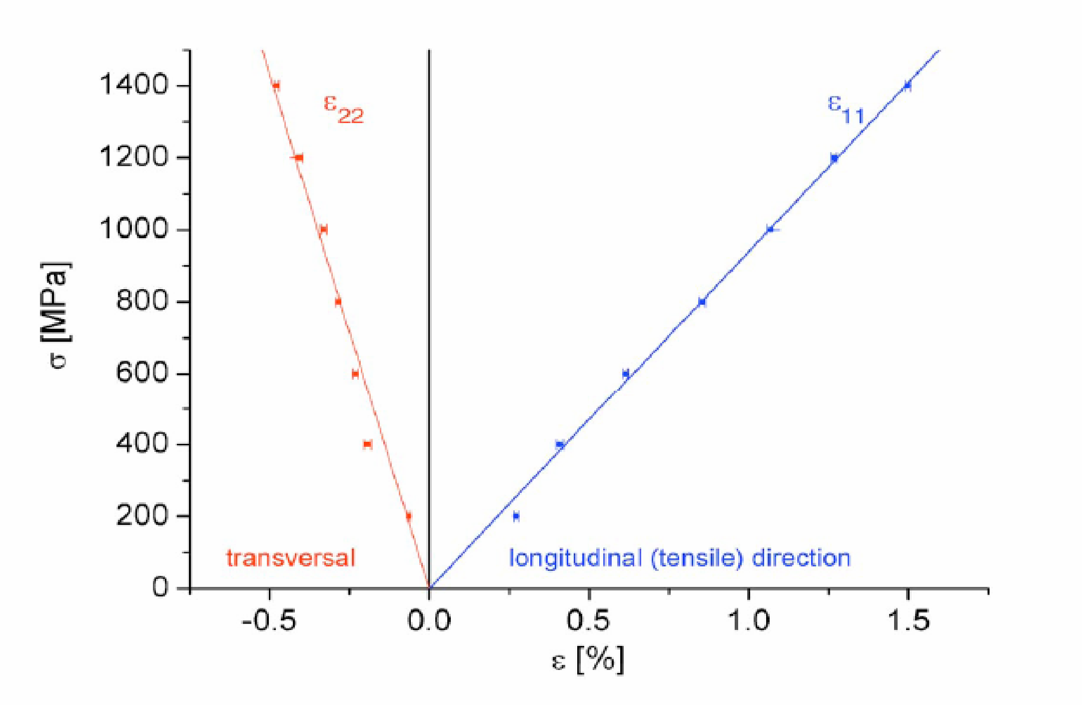

Crystalline metal

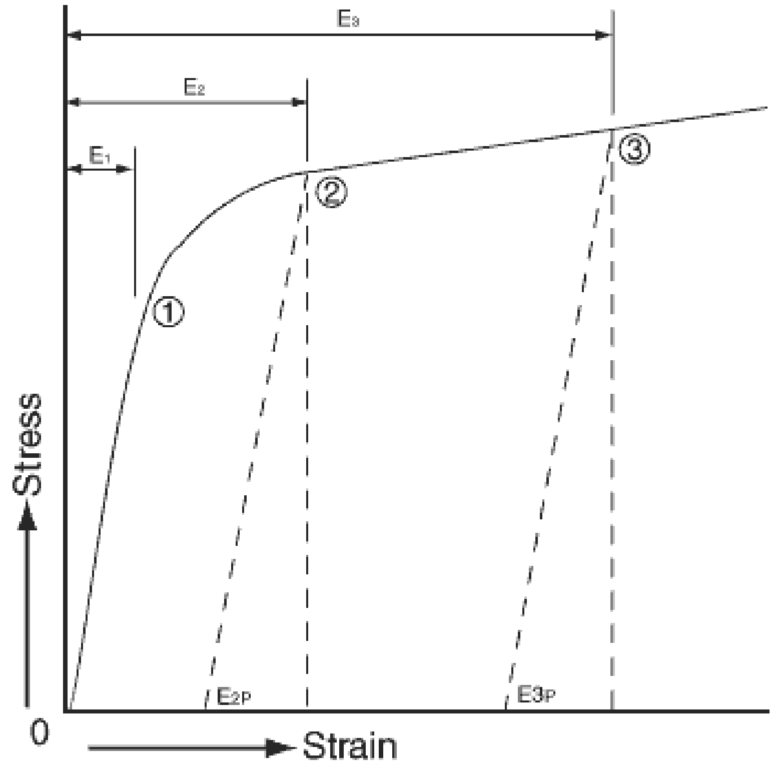

Relaxation phenomena and glass transition

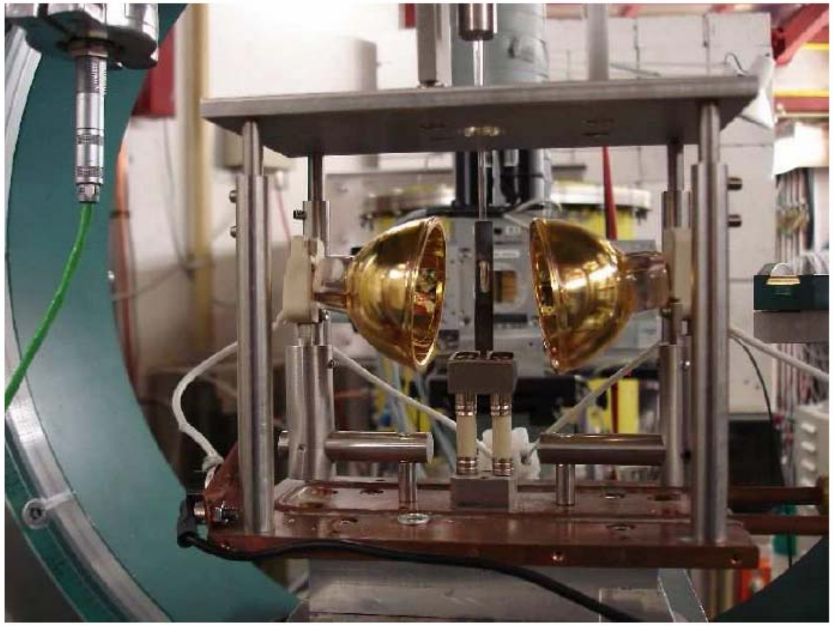

Figure 1: Detailed view showing infrared lamp furnace. Black tube sitting between two lamps supports capillary with the sample and serves as a heat condenser.

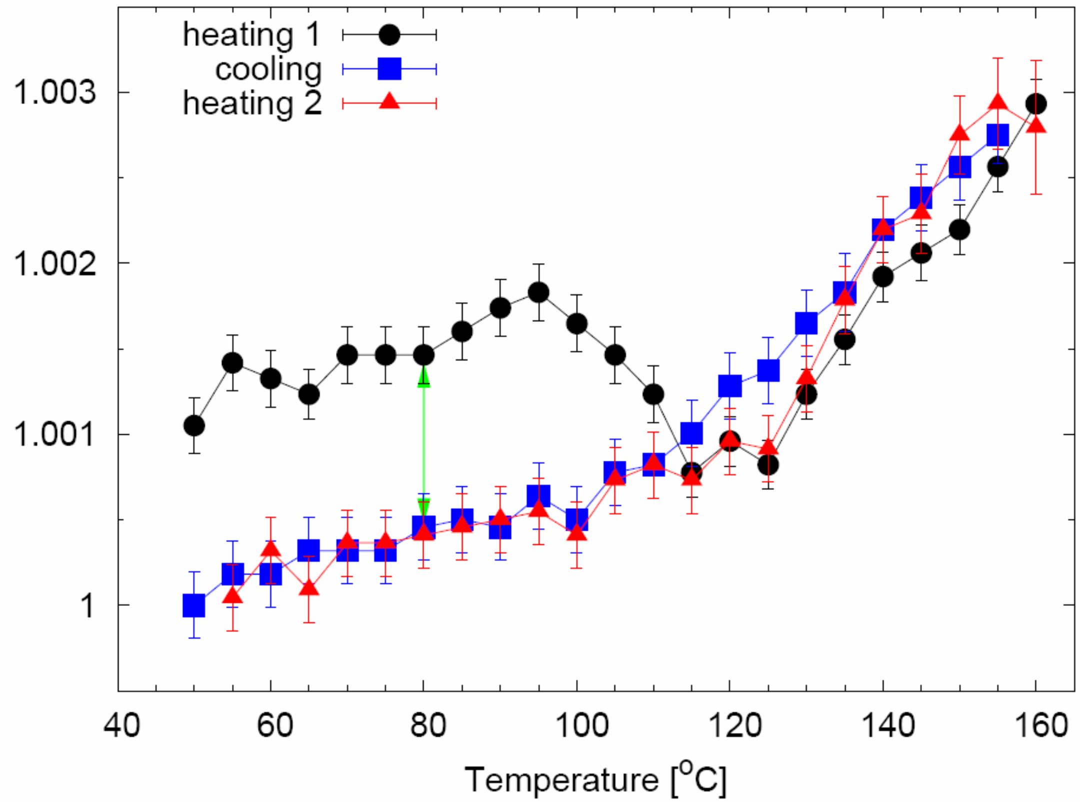

Relaxation phenomena and glass transition